RESEARCH PAPER

PCCP
www.rsc.org/pccp

A time-dependent Hartree–Fock approach for studying the electronic optical response of molecules in intense fields

Xiaosong Li,[a] Stanley M. Smith,[a] Alexei N. Markevitch,[bd] Dmitri A. Romanov,[cd] Robert J. Levis[bd] and H. Bernhard Schlegel*[a]

[a] *Department of Chemistry, Wayne State University, Detroit, MI 48202, USA*
[b] *Department of Chemistry, Temple University, Philadelphia, PA 19122, USA*
[c] *Department of Physics, Temple University, Philadelphia, PA 19122, USA*
[d] *Center for Advanced Photonics Research, Temple University, Philadelphia, PA 19122, USA*

Received 13th October 2004, Accepted 23rd November 2004
First published as an Advance Article on the web 10th December 2004

For molecules in high intensity oscillating electric fields, the time-dependent Hartree–Fock (TDHF) method is used to simulate the behavior of the electronic density prior to ionization. Since a perturbative approach is no longer valid at these intensities, the full TDHF equations are used to propagate the electronic density. A unitary transform approach is combined with the modified midpoint method to provide a stable and efficient algorithm to integrate these equations. The behavior of H_2^+ in an intense oscillating field computed using the TDHF method with a STO-3G basis set reproduces the analytic solution for the two-state coherent excitation model. For H_2 with a 6-311++G(d,p) basis set, the TDHF results are nearly indistinguishable from calculations using the full time-dependent Schrödinger equation. In an oscillating field of 3.17×10^{13} W cm^{-2} and 456 nm, the molecular orbital energies, electron populations, and atomic charges of H_2 follow the field adiabatically. As the field intensity is increased, the response becomes more complicated as a result of contributions from excited states. Simulations of N_2 show even greater complexity, yet the average charge still follows the field adiabatically.

I. Introduction

Intense femtosecond and picosecond lasers produce electric fields comparable with those sampled by valence electrons in a molecule. A number of non-perturbative phenomena have been observed and are typically called strong-field effects. Some of these phenomena, such as field tunneling and barrier-suppression ionization,[1–4] above-threshold ionization (ATI),[5,6] generation of higher-order harmonic emissions,[7–11] field-induced resonant enhancement of electronic absorption,[12–14] nonadiabatic multi-electron excitation,[15–18] require an understanding of the electronic wavefunction response to strong fields. Phenomena that involve nuclear motion, such as above-threshold dissociation,[19,20] bond softening and hardening,[19–21] charge-resonance-enhanced ionization,[22,23] Coulomb explosion of small[24,25] and large[26,27] molecules, cannot be understood without modeling of the complete electron-nuclear dynamics. Calculating the response of the electronic and nuclear wavefunctions to strong fields is essential for understanding, predicting and controlling these phenomena.

In a high intensity laser field, perturbative calculations are no longer valid to describe the electronic dynamics.[28–30] Advances in computer technology and numerical method have made it possible to perform numerical integrations of the full time-dependent Schrödinger equation (TDSE) for one- and two-electron systems for a length of time appropriate for strong-field experiments. For example, recent calculations of the electron dynamics of helium and argon by Muller *et al.* using TDSE demonstrate that the single-active electron approximation may accurately describe some aspects of strong-field atomic ionization.[31–33] For molecules, Thachuk, Ivanov and Wardlaw have employed the TDSE to propagate the electrons and classical dynamics for the nuclei to simulate ATI and dissociation in H_2^+ and HCl^+.[34,35] Bandrauk *et al.* used accurate numerical integrations of wavepackets to study the full quantum dynamics of H_2^+ and H_2 in intense laser fields.[36–47] These simulations provide insight into the laser-induced ionization and dissociation process, and explain multi-photon phenomena such as ATI and high-order harmonic generation.

Ivanov *et al.* have used an analytical semi-classical approach with two counter-propagating plane waves to describe the interaction of a model quantum system with strong oscillating fields.[48] This approach was successfully applied in theoretical studies of strong-field ionization dynamics of Rydberg atoms. There are, however, many aspects of strong field laser-molecule interaction that are definitely beyond the scope of the single-active electron approach. For example, Ivanov and co-workers have shown that non-adiabatic multi-electron (NME) dynamics is necessary to describe the ionization and dissociation of larger molecules in strong laser fields.[15–18] The computational simulation of such strong field phenomena require various levels of approximations to account for the multi-electron dynamics. Among the many formalisms for treating the interaction of a molecule and light, the time-dependent Hartree–Fock (TDHF) method is most widely used for investigations of laser-induced ionization,[40,49,50] computations of nonlinear susceptibilities,[51–57] and locating excited electronic states.[58,59] Though not as accurate, this method is much less demanding computationally than multiple configuration self-consistent field (MCSCF) based algorithms, because it avoids the explicit computations of the excited states by following the dynamics of a superposition state. The TDHF approach can be formulated in terms of either the wave function or the density matrix within a single Slater determinant framework. However, this type of formalism is still computationally expensive because electron dynamics have to be integrated using a small step size, and because large basis sets have to be employed to obtain good descriptions of the electronic response.

The computational cost can be reduced by using an effective Hamiltonian with a restricted basis and/or by considering a

DOI: 10.1039/b415849k

limited number of two-electron matrix elements. Such effective Hamiltonians are exemplified by the Hückel and the Su–Schrieffer–Heeger (SSH) Hamiltonians, the Pariser–Parr–Pople (PPP) model, valence effective Hamiltonians (VEH), complete neglect of differential overlap (CNDO), and intermediate neglect of differential overlap (INDO) models. In particular, the PPP Hamiltonian includes the Coulomb interaction among π electrons. It captures the essential electronic properties of the π systems, and has been employed in many studies of conjugated molecules.[54–56,60–63]

These approximate approaches are suitable for qualitative understanding of many essential features of electron dynamics. However, in the strong-field regime, they may be inadequate to describe the real electron (let alone electron-nuclear) dynamics of a complex multi-electron system. Our aim in this paper is to follow the electron dynamics in a molecule in intense laser fields prior to ionization, and not to simulate the ionization process itself. For larger molecules, we feel there is much to be learned in this regime that cannot be studied with current models. Although it would be highly desirable to model ionization as well, the accurate calculation of ionization rates is very demanding and is beyond the scope of the present paper. We present an efficient procedure for direct numerical integration of the time-dependent Hartree–Fock (TDHF) equations using the density matrix and atom-centered basis functions. Using diatomic molecules H_2^+, H_2 and N_2 we test the procedure by examining the time evolution of the molecular orbital energies, orbital populations, and the atomic charges. In a subsequent paper, the method will be used to study a series of larger molecules in intense fields.

II. Methodology

The time dependent Schrödinger equation (TDSE) is

$$i\hbar\frac{\partial\psi(t)}{\partial t} = \hat{H}(t)\psi(t). \tag{1}$$

The time dependent wavefunction can be expanded in terms of the eigenfunctions of the time independent, field free Hamiltonian, $\hat{H}_0\varphi_i = \omega_i\varphi_i$, and time dependent coefficients,

$$\psi(t) = \textstyle\sum_i C_i(t)\varphi_i. \tag{2}$$

The time dependent Schrödinger equation then reduces to a set of coupled differential equations for the coefficients,

$$\mathrm{i}\hbar\frac{\partial C_i(t)}{\partial t} = \sum_j H_{ij}(t)C_j(t). \tag{3}$$

where $H_{ij}(t) = \langle\varphi_i|\hat{H}|\varphi_j\rangle$. Except for very simple systems, such as H_2, this approach is not very practical, since the full expansion involves all excited states (*i.e.* full configuration interaction).

The time-dependent Hartree–Fock (TDHF) method starts with the time dependent Schrödinger equation, and restricts the wavefunction to a single Slater determinant but allows the one electron orbitals to be a function of time,

$$\psi(t) = \hat{A}[\phi_1(t)\phi_2(t)\cdots\phi_i(t)]. \tag{4}$$

The equations for the molecular orbitals $\phi_i(t)$ can be written in terms of the Fock operator,

$$\mathrm{i}\hbar\frac{\partial\phi_i(t)}{\partial t} = \hat{F}(t)\phi_i(t). \tag{5}$$

Correspondingly, for the one-particle density operator, $\boldsymbol{\Gamma}(t) = \sum_i^{\mathrm{occ}}\phi_i^*(t)\phi_i(t)$, one obtains

$$\mathrm{i}\hbar\frac{\mathrm{d}\boldsymbol{\Gamma}}{\mathrm{d}t} = \hat{F}(t)\boldsymbol{\Gamma}(t) - \boldsymbol{\Gamma}(t)\hat{F}(t) = \left[\hat{F}(t), \boldsymbol{\Gamma}(t)\right]. \tag{6}$$

The molecular orbitals can be expanded in terms of basis functions χ_μ,

$$\phi_i(t) = \sum_\mu c_{\mu,i}(t)\chi_\mu. \tag{7}$$

The density matrix can be constructed from the product of the molecular orbital coefficients

$$\boldsymbol{P}'_{\mu\nu}(t) = \sum_i c^*_{\mu,i}(t)c_{\nu,i}(t). \tag{8}$$

The corresponding Fock matrix is given by

$$\boldsymbol{F}'_{\mu\nu}(t) = \langle\chi_\mu|F(t)|\chi_\nu\rangle. \tag{9}$$

In general, the basis functions are not orthonormal, hence the overlap matrix

$$\boldsymbol{S}_{\mu\nu} = \langle\chi_\mu|\chi_\nu\rangle. \tag{10}$$

is not the identity. However, this basis can always be orthonormalized by means of Löwdin or Cholesky transformation methods. The density matrix and the Fock matrix are transformed from the AO basis ($\boldsymbol{P}'$ and $\boldsymbol{F}'$) into an orthonormal basis ($\boldsymbol{P}$ and $\boldsymbol{F}$) by a transformation matrix $\boldsymbol{V}$:

$$\boldsymbol{P} = \boldsymbol{V}\boldsymbol{P}'\boldsymbol{V}^{\mathrm{T}} \text{ and } \boldsymbol{F} = \boldsymbol{V}^{-\mathrm{T}}\boldsymbol{F}'\boldsymbol{V}^{-1}. \tag{11}$$

In the Löwdin orthonormalization method, $\boldsymbol{V} = \boldsymbol{S}^{1/2}$; in the Cholesky method, the upper triangular $\boldsymbol{V}$ is obtained by the decomposition $\boldsymbol{S} = \boldsymbol{V}^{\mathrm{T}}\boldsymbol{V}$.

In an orthonormal basis, the TDHF equation for the density matrix is

$$\mathrm{i}\frac{\mathrm{d}\boldsymbol{P}(t_i)}{\mathrm{d}t} = [\boldsymbol{F}(t_i), \boldsymbol{P}(t_i)]. \tag{12}$$

For the sake of simplicity, we will use atomic units from this point on.

In our simulations, we will use a linearly polarized and spatially homogeneous external field,

$$\boldsymbol{e}(\boldsymbol{r},t) \approx \boldsymbol{E}(t)\sin(\omega t + \varphi). \tag{13}$$

This is a good approximation for the laser field, because typical wavelengths are much larger than molecular dimensions.

The matrix elements of the field-dependent Hamiltonian in eqn. (3) can be expressed in terms of the field-free energies, ω_i, and transition dipole moments, $\boldsymbol{D}_{ij} = \langle\varphi_i|\boldsymbol{r}|\varphi_j\rangle$:

$$\begin{aligned} H_{ij}(t) &= \langle\varphi_i|\hat{H}|\varphi_j\rangle = \langle\varphi_i|\hat{H}_0|\varphi_j\rangle + \langle\varphi_i|\hat{\boldsymbol{r}}|\varphi_j\rangle E(t)\sin(\omega t + \varphi) \\ &= \omega_i\delta_{ij} + D_{ij}\exp(t). \end{aligned} \tag{14}$$

In a similar way, the field-dependent Fock matrix of eqn. (9) can be written in terms of the field-free Fock matrix $\boldsymbol{F}_0(t)$ and the dipole moment integrals in the AO basis, $\boldsymbol{d}'_{\mu\nu} = \langle\chi_\mu|\boldsymbol{r}|\chi_\nu\rangle$:

$$\boldsymbol{F}'(t) = \boldsymbol{F}'_0(t) + \boldsymbol{d}'\boldsymbol{e}(t) \tag{15}$$

Note, that the field-free Fock matrix also depends on time; this is due to the time dependence of the density matrix $\boldsymbol{P}$.

The time-dependent Hartree–Fock equation, eqn. (12), is an ordinary differential equation that can be solved numerically with a number of standard methods. However, low order methods such as Verlet and Runge–Kutta require a rather small step size to maintain the idempotency constraint on the density matrix, $\boldsymbol{P}\boldsymbol{P} = \boldsymbol{P}$. Symplectic integrators[64–76] are able to preserve the total phase space volume of the Hamiltonian system, but they also require small step sizes. Consequently, to integrate the TDHF equations efficiently, Micha has developed the "relax and drive" method.[77,78]

For the relax step, a new density matrix is obtained by a unitary transformation,

$$\boldsymbol{P}(t_i + \Delta t) = \boldsymbol{U}\boldsymbol{P}(t_i)\boldsymbol{U}^\dagger = \exp(\mathrm{i}\Delta t\boldsymbol{F}(t_i))\boldsymbol{P}(t_i)\exp(\mathrm{i}\Delta t\boldsymbol{F}(t_i)). \tag{16}$$

If the Fock matrix is expressed in its eigenspace,

$$\boldsymbol{C}^{\dagger}(t_i)\boldsymbol{F}(t_i)\boldsymbol{C}(t_i) = \boldsymbol{\varepsilon}(t_i), \quad (17)$$

the unitary transformation matrix, $\boldsymbol{U}$, can be written in terms of the eigenvectors $\boldsymbol{C}$ and eigenvalues $\boldsymbol{\varepsilon}$:

$$\boldsymbol{U} = \exp(\mathrm{i}\Delta t\boldsymbol{F}(t_i)) = \boldsymbol{C}(t_i)\exp(\mathrm{i}\Delta t\boldsymbol{\varepsilon}(t_i))\boldsymbol{C}^{\dagger}(t_i). \quad (18)$$

Since the matrix $\boldsymbol{U}$ is unitary, the idempotency constraint is preserved automatically for any size of time step. However, the Fock matrix changes during the time step, primarily due to interaction with the external field. The corresponding correction to the density matrix, $\Delta\boldsymbol{P}$, is calculated in the "drive" step as[77,78]

$$\Delta\boldsymbol{P} = \boldsymbol{U}\Delta'\boldsymbol{U}^{\dagger} \text{ where } \Delta' = \int [(\boldsymbol{F}(t')-\boldsymbol{F}(t_i)), \boldsymbol{U}\boldsymbol{P}(t_i)\boldsymbol{U}^{\dagger}]\mathrm{d}t'. \quad (19)$$

Note that most of the approaches operating with model Hamiltonians usually restrict themselves to an analogy of the relax step (for example, the quantum propagation toolkit approach[79,80]).

In order to develop a computationally efficient algorithm, we have tested some simple alternatives to the drive correction. If the external field is assumed to vary linearly during the time step and we use the field at the mid-point of the step to compute the Fock matrix and the transformation in eqn. (16), the drive correction in eqn. (19) should then be zero to first order in t.

$$\boldsymbol{U} = \exp(\mathrm{i}\Delta t(\boldsymbol{F}_0(t_i) + \boldsymbol{d}\boldsymbol{e}(t_i + \Delta t/2)) \text{ and } \boldsymbol{P}(t_{i+1}) = \boldsymbol{U}\boldsymbol{P}(t_i)\boldsymbol{U}^{\dagger} \quad (20)$$

Alternatively, we can take into account linear changes in both the density and the external field during the time step by computing the entire Fock matrix at the mid-point of the step, not just the field contribution. This corresponds to using a modified mid-point algorithm:

$$\boldsymbol{U} = \exp(2\mathrm{i}\Delta t\boldsymbol{F}(t_i)) \text{ and } \boldsymbol{P}(t_{i+1}) = \boldsymbol{U}\boldsymbol{P}(t_{i-1})\boldsymbol{U}^{\dagger}. \quad (21)$$

An alternative involves integration of the density in the interval from $t_{i-1/2}$ to $t_{i+1/2}$ using the Fock matrix at t_i, and extrapolating the density to t_{i+1} for the computation of the Fock matrix for the next step:

$$\boldsymbol{U} = \exp(\mathrm{i}\Delta t\boldsymbol{F}(t_i)) \text{ and } \boldsymbol{P}(t_{i+1/2}) = \boldsymbol{U}\boldsymbol{P}(t_{i-1/2})\boldsymbol{U}^{\dagger} \quad (22)$$

$$\boldsymbol{U}' = \exp(\mathrm{i}\Delta t\boldsymbol{F}(t_i)/2) \text{ and } \boldsymbol{P}(t_{i+1}) = \boldsymbol{U}'\boldsymbol{P}(t_{i+1/2})\boldsymbol{U}'^{\dagger}$$

This is similar to the approach used by Sun and Ruedenberg to integrate the equations for the steepest descent reaction paths.[81]

To characterize the behavior of a molecule in an intense field, we examine the evolution of the following specific molecular properties related to charge redistribution:

(i) the instantaneous dipole,

$$\boldsymbol{\mu}(t_i) = \sum_{\alpha} Z_{\alpha}\boldsymbol{R}_{\alpha} - \boldsymbol{d}' \cdot \boldsymbol{P}'(t_i); \quad (23)$$

(ii) the effective charge on atom α; for an atom centered basis set, this can be estimated by the Löwdin population analysis,

$$q_{\alpha} = Z_{\alpha} - \sum_{i\subset\alpha} P_{ii}(t), \quad (24)$$

where Z_{α} is the nuclear charge of the atom α, and the sum $\sum_{i\subset\alpha}P_{ii}(t)$ runs over the basis functions on this atom (P_{ii} is the ith diagonal element of the density matrix in the orthonormal basis);

(iii) the orbital occupation numbers, determined by projecting the time-dependent density matrix onto the initial orbitals,

$$n_k(t_i) = \boldsymbol{C}_k^{\dagger}(0)\boldsymbol{P}(t_i)\boldsymbol{C}_k(0), \quad (25)$$

where $\boldsymbol{C}_k(0)$ is the k-th eigenvector of the initial, field-free Fock matrix.

III. Results and discussion

Electronic dynamics in a strong time-varying electric field is simulated using the development version of GAUSSIAN series of program[82] with the addition of the algorithm presented here for evaluating the time-dependent Hartree–Fock equations using atom-centered basis functions and a modified mid-point, unitary transformation integration scheme (MMUT-TDHF). The initial conditions are the equilibrium bond lengths and the converged ground electronic state. The molecular axis is aligned with the direction of polarization of the electric field and the phase φ in eqn. (13) is chosen to be zero.

III.1. Two-state coherent excitation

Coherent excitation of a two-state system in a linearly polarized oscillating field is a classical example in the literature and in textbooks.[83–89] In particular, near the resonance this system exhibits a characteristic sinusoidal flow of complete population inversion (Rabi oscillation). The ground state of H_2^+ with a minimal basis set provides an ideal two-state problem. With the STO-3G basis set, the excitation energy ($D_0 \rightarrow D_1$), also referred to as Bohr frequency ω_0,[85] is 0.4764 au for H_2^+ at its minimum energy geometry (R_e = 1.0603 Å). The field-free Fock matrix of this one-electron system is time-independent. The applied field, shown in Fig. 1(a), has a constant envelope, $|\boldsymbol{E}(t)| = |\boldsymbol{E}_{\max}| = 0.05$ au, corresponding to an intensity of 8.75×10^{13} W cm^{-2}. Fig. 1(b) illustrates time evolution of electron population in orbitals 1 and 2, integrated using a step size of 0.2 au (4.838×10^{-3} fs) at the resonance frequency, ω_0. Our simulations yield sinusoidal oscillations of the electron population with the frequency $\tilde{\Omega} = 0.0567$ au. This result is in

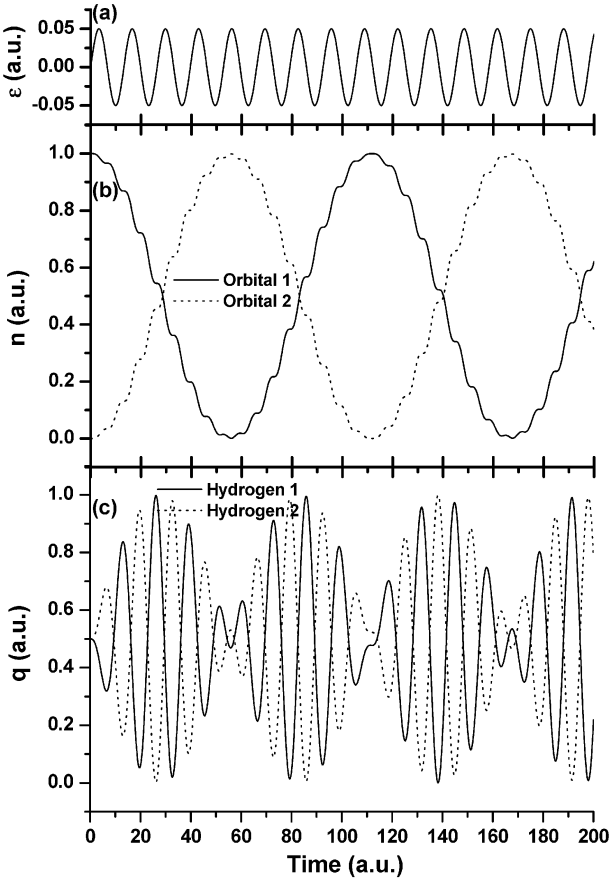

Fig. 1 TDHF simulation of H_2^+ in an oscillating electric field ($\boldsymbol{E}_{\max}$ = 0.05 au (8.75×10^{13} W cm^{-2}) and $\omega = 0.4764$ au.) using the STO-3G basis set: (a) electric field profile, (b) electron populations of orbitals and (c) Löwdin atomic charge analysis.

excellent agreement with the analytic solution[85]

$$\tilde{\Omega} = \sqrt{\Omega^2 + (\omega - \omega_0)^2}, \qquad (26)$$

where the Rabi oscillation frequency $\Omega = |d||E_{max}|/\hbar$ is 0.056 82 au for the H_2^+ with STO-3G basis set. Fig. 1(c) shows the evolution of the effective atomic charges obtained from the Löwdin population analysis. As can be seen from the Figure, the H_2^+ molecule oscillates between complete covalent and ionic bond configurations.

III.2. H_2 in intense laser fields

The electron optical responses of the H_2 and its ions have been studied extensively for decades,[36–47,90–96] because they are computationally simple and can be solved analytically at some levels of approximation. Since there is such a wealth of information on H_2 from the work by Bandrauk *et al.* and other groups using wave packet dynamics,[36–41] we examined hydrogen molecule in a strong oscillating field as a test of our method.

For the optical response of H_2 in intense laser fields, perturbative calculations are not valid because the canonical molecular orbitals no longer differ from the ground state configuration by only a small amount. In a non-perturbative approach, the field-free Fock matrix $\boldsymbol{F}$ is constructed using the time-dependent density matrix $\boldsymbol{P}$, and therefore is also time-dependent. For a better description of the electronic excitation levels of H_2, we have used larger basis sets than for the two-state coherent excitation (Section III.1). In the first series of tests, molecular orbitals are expanded in 14 Gaussian type functions using the 6-311++G(d,p) split-valence basis set with diffuse and polarization functions. This corresponds to four s-type functions and one set of p-type functions on each hydrogen. The field envelope $|\boldsymbol{E}(t)|$ is linearly increased with time to a maximum value of $|\boldsymbol{E}_{max}|$ at the end of the first cycle and remains at $|\boldsymbol{E}_{max}|$ for one cycle and then decreases to zero by the end of the next cycle, as shown in Fig. 2(a).

$$\begin{array}{rll} \boldsymbol{E}(t) = (\omega t/2\pi)\boldsymbol{E}_{max} & \text{for} & 0 \le t \le 2\pi/\omega \\ \boldsymbol{E}(t) = \boldsymbol{E}_{max} & \text{for} & 2\pi/\omega \le t \le 4\pi/\omega \\ \boldsymbol{E}(t) = (3 - \omega t/2\pi)\boldsymbol{E}_{max} & \text{for} & 4\pi/\omega \le t \le 6\pi/\omega \\ \boldsymbol{E}(t) = 0 & \text{for} & t<0 \text{ and } t>6\pi/\omega \end{array} \qquad (27)$$

This envelope will be used for the remainder of the paper.

Fig. 2 shows the electron optical response of the H_2 at the equilibrium geometry ($R_e = 0.7354$ Å at HF/6-311++G(d,p)) in a 456 nm ($\omega = 0.10$ au) laser field. The maximum field intensity is 3.17×10^{13} W cm^{-2} ($\boldsymbol{E}_{max} = 0.03$ au). Fig. 2(b) shows the orbital energy profiles of the lowest four orbitals, $1\sigma_g$, $1\sigma_u$, $2\sigma_g$ and $2\sigma_u$. The bonding orbital ($1\sigma_g$) of H_2 is relatively insensitive to the applied field, while the energies of $1\sigma_u$ and $2\sigma_g$ orbitals oscillate significantly, crossing several times during the simulation.

Fig. 2(c) shows the electron population in the lowest four molecular orbitals. In this simulation, we do not see any significant population in orbitals higher than $2\sigma_g$. While the field is on, the depopulation of the ground state barely reaches 0.16%, while the population of $2\sigma_g$ is less than 0.01%. This particular population dynamics is due to the characteristics of dipole transitions in the system. The lowest dipole-allowed singlet excitations of H_2 are $S_0 \rightarrow S_1$ and $S_0 \rightarrow S_3$. Since these excitations are combinations of the $1\sigma_g \rightarrow 1\sigma_u$ and $1\sigma_g \rightarrow 2\sigma_u$ transitions, this results in some population of the $1\sigma_u$ and $2\sigma_u$ orbitals. The $S_0 \rightarrow S_2$ excitation corresponds to the $1\sigma_g$ to $2\sigma_g$ transition that is not allowed in the dipole approximation. Hence, there is almost no population in $2\sigma_g$ orbital. When the field falls back to zero, the populations return to their ground state values, as expected for an adiabatic response to the field.

The fluctuation of the effective atomic charge caused by the oscillation of the molecular orbital populations is shown in Fig. 2(d). Compared to the case of H_2^+, where the effective atomic charge oscillates between +1 and –1 (see Fig. 1(c)), the charge fluctuations in this off-resonnance case for H_2 are much smaller, only ±0.08. This degree of polarization of H_2 is in good agreement with the charge shift calculated with a static field of the same magnitude.

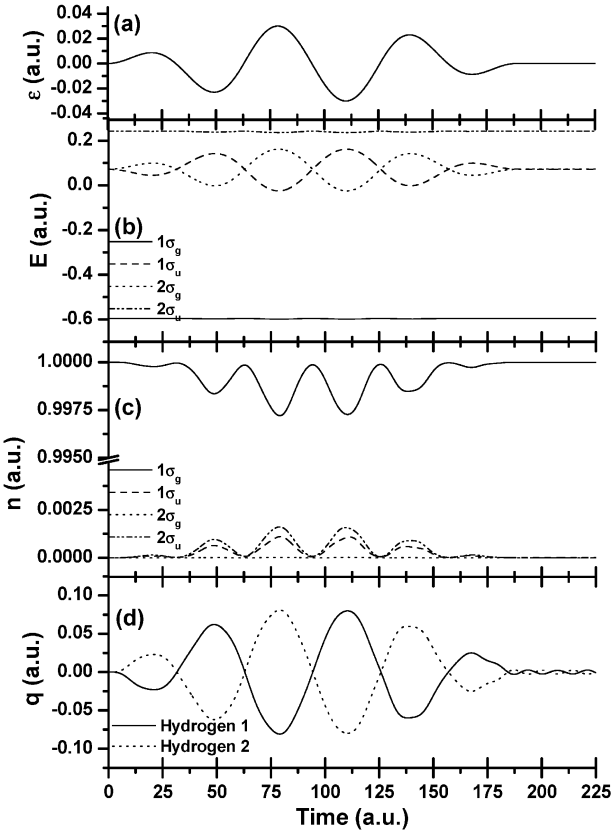

Fig. 2 TDHF simulation for H_2 in an oscillating electric field ($\boldsymbol{E}_{max} = 0.03$ au (3.17×10^{13} W cm^{-2}) and $\omega = 0.10$ au (456 nm)) using the 6-311++G(d,p) basis set: (a) electric field profile, (b) energies of the lowest four orbitals, (c) electron populations of the lowest four orbitals and (d) Löwdin atomic charge analysis.

As can be seen in Fig. 2 with $\boldsymbol{E}_{max} = 0.03$ au., the electron response follows the external field adiabatically: when the field passes through zero and after the field is turned off, the electrons populate only the ground state orbital and the effective charge on each hydrogen atom is close to zero. Similar adiabatic behavior of H_2 at near-equilibrium internuclear distances was obtained in numerical simulations by Bandrauk *et al.*[36]

When the field intensity is increased to 1.72×10^{14} W cm^{-2} ($|\boldsymbol{E}_{max}| = 0.07$ au), electronic response of H_2 is more complex, as shown in Fig. 3, and there is a potential for some ionization. The Keldysh parameter[1] (γ) can be used to determine the ionization mechanism for a given electric field strength and laser frequency: $\gamma \gg 1$ corresponds to the multi-photon ionization regime including above threshold ionization (ATI), $\gamma \cong 1$ corresponds to the tunneling regime, and $\gamma \ll 1$ corresponds to the over the barrier ionization. The Keldysh parameter is calculated by

$$\gamma = \sqrt{\frac{|I_p|}{2U_p}} \text{ and } U_p = \left(\frac{F_0}{2\omega}\right) \qquad (28)$$

where I_p is the ionization potential, U_p is the ponderomotive potential or quiver energy of the electron and F_0 and ω are the amplitude and angular frequency of the laser field all in atomic units. A maximum field intensity of 1.72×10^{14} W cm^{-2} yields a Keldysh parameter of $\gamma = 1.52$ indicating that we are not in

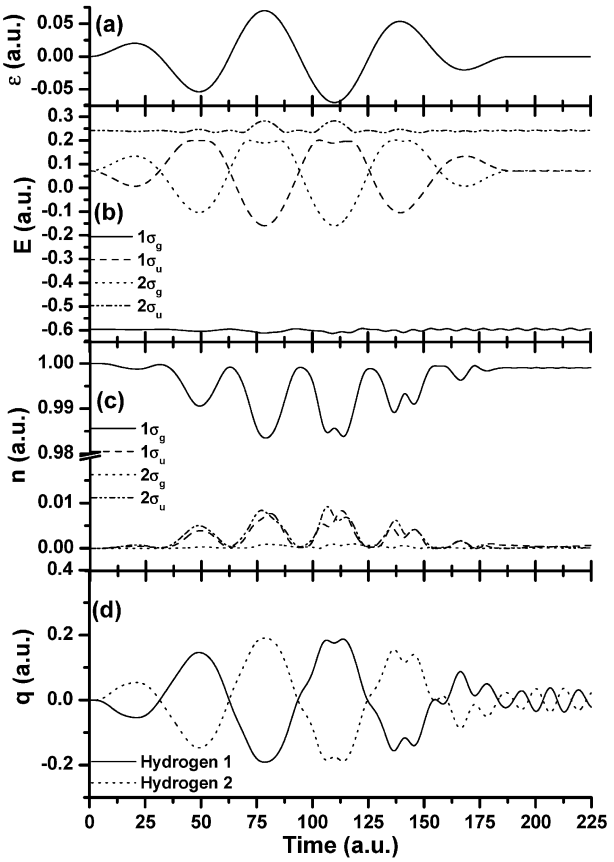

Fig. 3 TDHF simulation for H_2 in an oscillating electric field ($\boldsymbol{E}_{max}$ = 0.07 au (1.72 × 10^{14} W cm^{-2}) and ω = 0.10 au (456 nm)) using the 6-311++G(d,p) basis set: (a) electric field profile, (b) energies of the lowest four orbitals, (c) electron populations of the lowest four orbitals and (d) Löwdin atomic charge analysis.

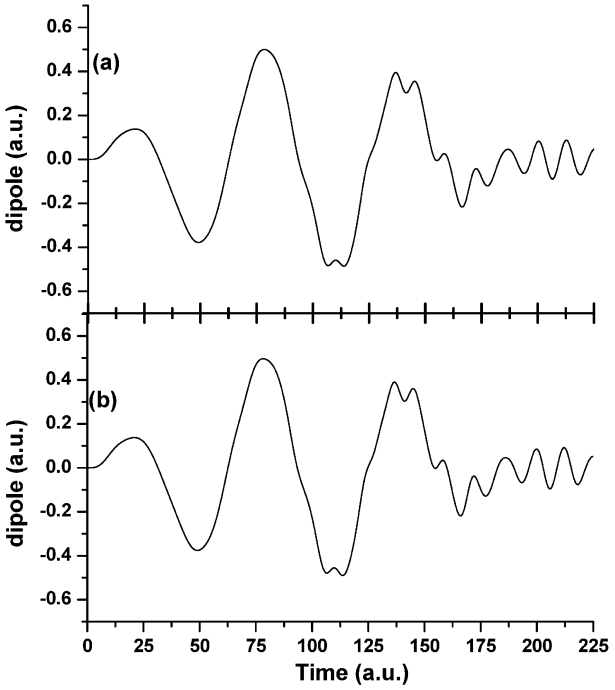

Fig. 4 Instantaneous dipole for H_2 in an oscillating electric field ($\boldsymbol{E}_{max}$ = 0.07 au (1.72 × 10^{14} W cm^{-2}) and ω = 0.10 au (456 nm)) using the 6-311++G(d,p) basis set: (a) TDHF simulation, eqn. (12) and (b) TDSE simulation, eqn. (3).

the over the barrier regime. The experimental ionization rate of H_2 is estimated to be *ca.* 0.03 fs^{-1} at this field strength. Thus, ionization should not be significant for the short duration of the pulse. Fig. 3(b) shows that the field causes crossings between the energies of the $1\sigma_u$ and $2\sigma_g$ orbitals and avoided crossings between the $1\sigma_u$ and $2\sigma_u$ orbitals. The orbital populations, Fig. 3(c), vary appreciably: the depopulation of the ground state reaches 4% and the population of $2\sigma_g$ approaches 0.5%. However, as in the case of weaker fields (Fig. 2), only the $1\sigma_g$, $1\sigma_u$, $2\sigma_g$ and $2\sigma_u$ orbitals are involved in electronic transitions and no significant population is seen in higher orbitals. The population of $2\sigma_g$ cannot result directly from the forbidden $S_0 \rightarrow S_2$ transition. This suggests that the dipole-allowed transitions from $1\sigma_u$ to $2\sigma_g$ and from $2\sigma_u$ to $2\sigma_g$ are responsible for the population in the $2\sigma_g$ orbital. When the field returns to zero, small oscillations of the charge continue. These oscillation results from the superposition of excited states that are populated during the pulse. These states remain populated after the pulse and cause the charge oscillations in observed in Fig. 3(d) and the fluctuations in the dipole moment shown in Fig. 4.

To confirm the results of the TDHF calculations on the hydrogen molecule, we compared them with a direct numerical integration of the full time-dependent Schrödinger equation (TDSE) using an expansion in terms of excited states (hydrogen molecule is small enough for such a simulation). Fig. 4(b) shows the evolution of the instantaneous dipole for H_2 with the time-dependent Schrödinger equation, obtained by integrating eqn. (3) for H_2 using the ground state and the six lowest excited states. The necessary energies and transition dipoles were calculated using singles and doubles configuration interaction and the 6-311++G(d,p) basis set. The same results are obtained using only the four lowest excited states (but not with fewer than four states). It is clear from comparing Fig. 4(a) and 4(b) that the results of TDHF simulation are almost indistinguishable from the TDSE results. This directly validates our approach and implicitly supports the interpretation of its results given in the preceding paragraph.

In the second series of tests on H_2, we have used a much larger basis set. The augmented, correlation consistent, polarized valence triple zeta (aug-ccpVTZ) basis set of Dunning and co-workers[97,98] was supplemented with three sets of diffuse sp shells per atom. With this basis set each hydrogen atom has four contracted s functions with Gaussian exponents ranging from 33.87 to 0.02526, three sets of uncontracted p functions with exponents 1.407, 0.388 and 0.102, two sets of d functions with exponent 1.057 and 0.247, and three sets of diffuse sp shells with exponents 0.0100, 0.0050 and 0.0025, for a total of 70 functions for H_2. The results of the TDHF simulations for H_2 with $\boldsymbol{E}_{max}$ = 0.07 au are shown in Fig. 5 (the TDSE results simulated with 68 excited states are comparable). While the populations and instantaneous dipole show some additional, higher frequency oscillations, the overall features are similar to TDHF/6-311++G(d,p) calculations with the same field strength. This suggests that the smaller basis set may be adequate to qualitatively model the response of H_2 to the present pulse shape and intensity.

III.3 N_2 in intense laser fields

The results of a TDHF simulation of the electronic response of a heavier molecule, N_2, interacting with a 456 nm (ω = 0.10 au.) laser field are shown in Fig. 6. Here, we use 6-311++G(d,p) basis set; the N_2 molecule is taken in its equilibrium geometry, with R_e = 1.0706 Å. The maximum field intensity is 1.72 × 10^{14} W cm^{-2} ($\boldsymbol{E}_{max}$ = 0.07 au), yielding a Keldysh parameter of γ = 1.53. The adiabatic response of the electrons to the time-dependent electric field is complicated by the onset of a higher-period oscillation pattern, similar to the case of the H_2 molecule seen in Figs. 3–5.

With the simple relaxation method, eqn. (16), the results of integration with the step size of 0.01 au are identical to those

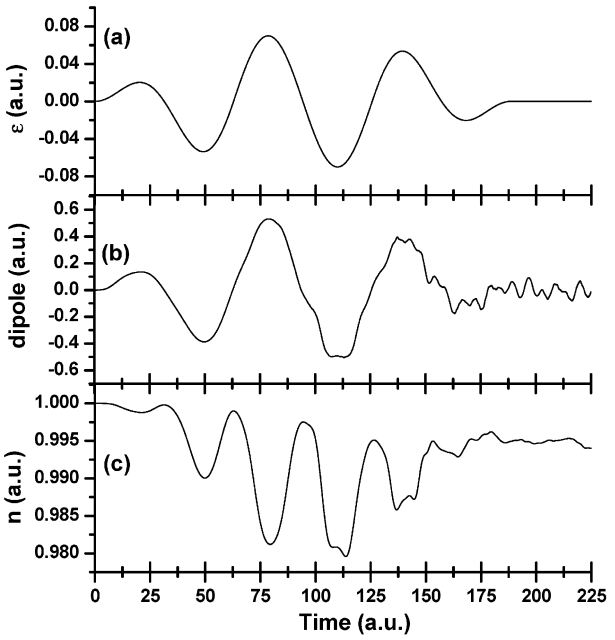

Fig. 5 TDHF simulation for H_2 in an oscillating electric field (E_{max} = 0.07 au (1.72×10^{14} W cm^{-2}) and ω = 0.10 au (456 nm)) using the aug-ccpVTZ basis set supplemented with 3 sets of diffuse sp functions on each atom: (a) electric field profile, (b) the instantaneous dipole and (c) electron population of the $1\sigma_g$ orbital of the field free ground state.

with a step size of 0.001 au, indicating excellent control of integration errors and numerical noise. The improved method of eqn. (20) takes into account the change in the external field during the time step and yields the same results as obtained from eqn. (16). However, this method does not allow one to use significantly larger time steps. Employing the modified midpoint approach, eqn. (21), enables the step size to be increased by a factor of 10 and improves the stability of the integration. In particular, for N_2, the modified midpoint approach using a step size of 0.1 au yields results identical to those obtained with simple relaxation method using step sizes of 0.01 and 0.001 au. Although the Sun–Ruedenberg approach, eqn. (22), also allows a ~ten-fold increase in the step size over simple relaxation method, we prefer the modified midpoint approach, because eqn. (21) requires only one propagation step. For smoothly varying external fields, this approach serves as an attractive alternative to the "relax and drive" method, and performs with comparable efficiency.

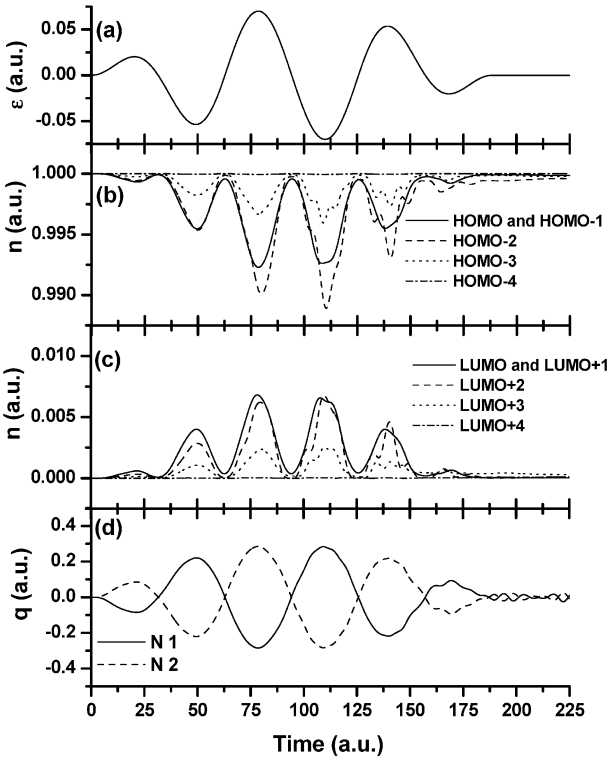

Fig. 6 TDHF simulation for N_2 in an oscillating electric field (E_{max} = 0.07 au (1.72×10^{14} W cm^{-2}) and ω = 0.10 au (456 nm)) using the 6-311++G(d,p) basis set: (a) electric field profile, (b) electron populations of the highest five ground state occupied orbitals, (c) electron populations of the lowest five ground state unoccupied orbitals and (d) Löwdin atomic charge analysis.

IV. Conclusion

In the current study, we have examined a few diatomic molecules subjected to strong oscillating fields and calculated the response of the electron density prior to ionization. We employed a direct integration of the time-dependent Hartree–Fock equation using atom-centered basis functions and a unitary transformation approach with a modified midpoint algorithm (MMUT-TDHF). Compared to the simple unitary transform method, the presented algorithm can be used with a larger step size, while still maintaining very good control of numerical noise and integration errors.

For the simple two-state system of H_2^+ in a minimal basis, the TDHF calculations yield the same Rabi oscillations of the state population as the analytic solution. When TDHF is used to simulate H_2 in a field of 3.17×10^{13} W cm^{-2} and 456 nm, the molecular orbital energies, electron populations and atomic charges follow the field adiabatically. For more intense fields, the orbital energies, populations and charges show a more complicated pattern on top of the adiabatic response. To validate the TDHF approach, the calculations were compared to integrations using the time dependent Schrödinger equation. Simulations of N_2 in the field of the same intensity and frequency also show a complex pattern evolving on top of adiabatic oscillations. The MMUT-TDHF method is computationally efficient enough to be applied to larger systems which will be studied in forthcoming papers.

Acknowledgements

This work was supported by the National Science Foundation (CHE 0131157 to HBS, CHE 0313967 to RJL), Gaussian Inc., and DoD MURI grant as administered by the Army Research Office.

References

1 L. V. Keldysh, *Sov. Phys. JETP*, 1965, **20**, 1307.
2 M. V. Ammosov, N. B. Delone and V. P. Krainov, *Sov. Phys. JETP*, 1986, **64**, 1191.
3 M. J. DeWitt and R. J. Levis, *Phys. Rev. Lett.*, 1998, **81**, 5101.
4 R. J. Levis and M. J. DeWitt, *J. Phys. Chem. A*, 1999, **103**, 6493.
5 J. H. Eberly, J. Javanainen and K. Rzazewski, *Phys. Rep.-Rev. Sec. Phys. Lett.*, 1991, **204**, 331.
6 H. G. Muller, P. H. Bucksbaum, D. W. Schumacher and A. Zavriyev, *J. Phys. B*, 1990, **23**, 2761.
7 T. Zuo and A. D. Bandrauk, *J. Nonlinear Opt. Phys. Mater.*, 1995, **4**, 533.
8 A. McPherson, G. Gibson, H. Jara, U. Johann, T. S. Luk, I. A. McIntyre, K. Boyer and C. K. Rhodes, *J. Opt. Soc. Am. B*, 1987, **4**, 595.
9 A. Lhuillier, K. J. Schafer and K. C. Kulander, *J. Phys. B*, 1991, **24**, 3315.
10 P. Salieres, P. Antoine, A. de Bohan and M. Lewenstein, *Phys. Rev. Lett.*, 1998, **81**, 5544.
11 P. Antoine, A. Lhuillier, M. Lewenstein, P. Salieres and B. Carre, *Phys. Rev. A*, 1996, **53**, 1725.
12 R. R. Freeman, P. H. Bucksbaum, H. Milchberg, S. Darack, D. Schumacher and M. E. Geusic, *Phys. Rev. Lett.*, 1987, **59**, 1092.

13 M. P. Deboer and H. G. Muller, *Phys. Rev. Lett.*, 1992, **68**, 2747.
14 G. N. Gibson, R. R. Freeman and T. J. McIlrath, *Phys. Rev. Lett.*, 1992, **69**, 1904.
15 M. Lezius, V. Blanchet, D. M. Rayner, D. M. Villeneuve, A. Stolow and M. Y. Ivanov, *Phys. Rev. Lett.*, 2001, **86**, 51.
16 M. Lezius, V. Blanchet, M. Y. Ivanov and A. Stolow, *J. Chem. Phys.*, 2002, **117**, 1575.
17 A. N. Markevitch, S. M. Smith, D. A. Romanov, H. B. Schlegel, M. Y. Ivanov and R. J. Levis, *Phys. Rev. A*, 2003, **68**, 011402.
18 A. N. Markevitch, D. A. Romanov, S. M. Smith, H. B. Schlegel, M. Y. Ivanov and R. J. Levis, *Phys. Rev. A*, 2004, **69**, 013401.
19 P. H. Bucksbaum, A. Zavriyev, H. G. Muller and D. W. Schumacher, *Phys. Rev. Lett.*, 1990, **64**, 1883.
20 A. Zavriyev, P. H. Bucksbaum, H. G. Muller and D. W. Schumacher, *Phys. Rev. A*, 1990, **42**, 5500.
21 L. J. Frasinski, J. H. Posthumus, J. Plumridge, K. Codling, P. F. Taday and A. J. Langley, *Phys. Rev. Lett.*, 1999, **83**, 3625.
22 T. Seideman, M. Y. Ivanov and P. B. Corkum, *Phys. Rev. Lett.*, 1995, **75**, 2819.
23 T. Zuo and A. D. Bandrauk, *Phys. Rev. A*, 1995, **52**, R2511.
24 C. Cornaggia, J. Lavancier, D. Normand, J. Morellec, P. Agostini, J. P. Chambaret and A. Antonetti, *Phys. Rev. A*, 1991, **44**, 4499.
25 C. Cornaggia, M. Schmidt and D. Normand, *J. Phys. B*, 1994, **27**, L123.
26 V. R. Bhardwaj, P. B. Corkum and D. M. Rayner, *Phys. Rev. Lett.*, 2003, **91**.
27 A. N. Markevitch, D. A. Romanov, S. M. Smith and R. J. Levis, *Phys. Rev. Lett.*, 2004, **92**.
28 *Atomic and Molecular Processes with Short Intense Laser Pulses, NATO ASI B171*, ed. A. D. Bandrauk, Plenum Press, 1988.
29 *Coherence Phenomena in Atoms and Molecules in Laser Fields, NATO ASI B278*, ed. A. D. Bandrauk and S. C. Wallace, Plenum Press, 1992.
30 A. D. Bandrauk, *Molecules in Laser Fields*, Marcel Dekker, 1993.
31 H. G. Muller, *Phys. Rev. Lett.*, 1999, **83**, 3158.
32 M. J. Nandor, M. A. Walker, L. D. Van Woerkom and H. G. Muller, *Phys. Rev. A*, 1999, **60**, R1771.
33 H. G. Muller, *Phys. Rev. A*, 1999, **60**, 1341.
34 M. Thachuk, M. Y. Ivanov and D. M. Wardlaw, *J. Chem. Phys.*, 1998, **109**, 5747.
35 M. Thachuk, M. Y. Ivanov and D. M. Wardlaw, *J. Chem. Phys.*, 1996, **105**, 4094.
36 K. Harumiya, H. Kono, Y. Fujimura, I. Kawata and A. D. Bandrauk, *Phys. Rev. A*, 2002, **66**, 43403.
37 T. D. G. Walsh, F. A. Ilkov, S. L. Chin, F. Chateauneuf, T. T. Nguyen-Dang, S. Chelkowski, A. D. Bandrauk and O. Atabek, *Phys. Rev. A*, 1998, **58**, 3922.
38 H. T. Yu, T. Zuo and A. D. Bandrauk, *Phys. Rev. A*, 1996, **54**, 3290.
39 A. Talebpour, K. Vijayalakshmi, A. D. Bandrauk, T. T. Nguyen-Dang and S. L. Chin, *Phys. Rev. A*, 2000, **62**, 42708.
40 M. Lein, T. Kreibich, E. K. U. Gross and V. Engel, *Phys. Rev. A*, 2002, **65**, 033403.
41 I. Kawata, A. D. Bandrauk, H. Kono and Y. Fujimura, *Laser Phys.*, 2001, **11**, 188.
42 A. D. Bandrauk and H. Z. Lu, *Phys. Rev. A*, 2000, **62**, 53406.
43 A. D. Bandrauk, S. Chelkowski and J. Levesque, *Laser Phys.*, 2002, **12**, 468.
44 A. D. Bandrauk and S. Chelkowski, *Phys. Rev. Lett.*, 2000, **84**, 3562.
45 S. Chelkowski, M. Zamojski and A. D. Bandrauk, *Phys. Rev. A*, 2001, **63**, 23409.
46 H. T. Yu, A. D. Bandrauk and V. Sonnad, *J. Math. Chem.*, 1994, **15**, 287.
47 T. Zuo and A. D. Bandrauk, *Phys. Rev. A*, 1995, **51**, R26.
48 M. Y. Ivanov, O. V. Tikhonova and M. V. Fedorov, *Phys. Rev. A*, 1998, **58**, R793.
49 K. C. Kulander, *Phys. Rev. A*, 1987, **36**, 2726.
50 K. C. Kulander, *Phys. Rev. A*, 1987, **35**, 445.
51 H. Sekino and R. J. Bartlett, *J. Chem. Phys.*, 1986, **85**, 976.
52 H. Sekino and R. J. Bartlett, *Int. J. Quantum Chem.*, 1992, **43**, 119.
53 A. Takahashi and S. Mukamel, *J. Chem. Phys.*, 1994, **100**, 2366.
54 G. H. Chen and S. Mukamel, *J. Chem. Phys.*, 1995, **103**, 9355.
55 G. H. Chen and S. Mukamel, *J. Phys. Chem.*, 1996, **100**, 11080.
56 G. H. Chen and S. Mukamel, *Chem. Phys. Lett.*, 1996, **258**, 589.
57 G. H. Chen, S. Mukamel, D. Beljonne and J. L. Bredas, *J. Chem. Phys.*, 1996, **104**, 5406.
58 D. A. Micha, *Int. J. Quantum Chem.*, 1996, **60**, 109.
59 E. V. Tsiper, V. Chernyak, S. Tretiak and S. Mukamel, *Chem. Phys. Lett.*, 1999, **302**, 77.
60 S. Mukamel, S. Tretiak, T. Wagersreiter and V. Chernyak, *Science*, 1997, **277**, 781.
61 S. Tretiak and S. Mukamel, *Chem. Rev.*, 2002, **102**, 3171.
62 M. Suzuki and S. Mukamel, *J. Chem. Phys.*, 2003, **119**, 4722.
63 M. Suzuki and S. Mukamel, *J. Chem. Phys.*, 2004, **120**, 669.
64 S. K. Gray, D. W. Noid and B. G. Sumpter, *J. Chem. Phys.*, 1994, **101**, 4062.
65 S. K. Gray and J. M. Verosky, *J. Chem. Phys.*, 1994, **100**, 5011.
66 S. K. Gray and D. E. Manolopoulos, *J. Chem. Phys.*, 1996, **104**, 7099.
67 D. E. Manolopoulos and S. K. Gray, *J. Chem. Phys.*, 1995, **102**, 9214.
68 J. Candy and W. Rozmus, *J. Comput. Phys.*, 1991, **92**, 230.
69 M. P. Calvo and J. M. Sanzserna, *SIAM J. Sci. Comput.*, 1993, **14**, 936.
70 W. G. Hoover, O. Kum and N. E. Owens, *J. Chem. Phys.*, 1995, **103**, 1530.
71 R. Bigwood and M. Gruebele, *Chem. Phys. Lett.*, 1995, **233**, 383.
72 R. I. McLachlan and P. Atela, *Nonlinearity*, 1992, **5**, 541.
73 R. I. McLachlan and C. Scovel, *J. Nonlinear Sci.*, 1995, **5**, 233.
74 R. D. Ruth, *IEEE Trans. Nucl. Sci.*, 1983, **30**, 2669.
75 J. M. Sanzserna and M. P. Calvo, *Int. J. Mod. Phys. C-Phys. Comput.*, 1993, **4**, 385.
76 J. M. SanzSerna and A. Portillo, *J. Chem. Phys.*, 1996, **104**, 2349.
77 D. A. Micha, *J. Phys. Chem. A*, 1999, **103**, 7562.
78 D. A. Micha, *Adv. Quantum Chem.*, 1999, **35**, 317.
79 F. L. Yip, D. A. Mazziotti and H. Rabitz, *J. Phys. Chem. A*, 2003, **107**, 7264.
80 F. L. Yip, D. A. Mazziotti and H. Rabitz, *J. Chem. Phys.*, 2003, **118**, 8168.
81 J. Q. Sun and K. Ruedenberg, *J. Chem. Phys.*, 1993, **99**, 5257.
82 M. J. Frisch, G. W. Trucks, H. B. Schlegel, G. E. Scuseria, M. A. Robb, J. R. Cheeseman, J. A. Montgomery, T. Vreven, K. N. Kudin, J. C. Burant, J. M. Millam, S. Iyengar, J. Tomasi, V. Barone, B. Mennucci, M. Cossi, G. Scalmani, N. Rega, G. A. Petersson, H. Nakatsuji, M. Hada, M. Ehara, K. Toyota, R. Fukuda, J. Hasegawa, M. Ishida, T. Nakajima, Y. Honda, O. Kitao, H. Nakai, M. Klene, X. Li, J. E. Knox, H. P. Hratchian, J. B. Cross, C. Adamo, J. Jaramillo, R. Gomperts, R. E. Stratmann, O. Yazyev, A. J. Austin, R. Cammi, C. Pomelli, J. Ochterski, P. Y. Ayala, K. Morokuma, G. A. Voth, P. Salvador, J. J. Dannenberg, V. G. Zakrzewski, S. Dapprich, A. D. Daniels, M. C. Strain, Ö. Farkas, D. K. Malick, A. D. Rabuck, K. Raghavachari, J. B. Foresman, J. V. Ortiz, Q. Cui, A. G. Baboul, S. Clifford, J. Cioslowski, B. B. Stefanov, G. Liu, A. Liashenko, P. Piskorz, I. Komaromi, R. L. Martin, D. J. Fox, T. Keith, M. A. Al-Laham, C. Y. Peng, A. Nanayakkara, M. Challacombe, P. M. W. Gill, B. Johnson, W. Chen, M. W. Wong, J. L. Andres, C. Gonzalez, E. S. Replogle and J. A. Pople, *GAUSSIAN 03*, Pittsburgh PA, 2003.
83 D. R. Dion and J. O. Hirschfelder, *Adv. Chem. Phys.*, 1976, **35**, 265.
84 J. H. Shirley, *Phys. Rev., Sect. B*, 1965, **138**, 979.
85 B. W. Shore, *The Theory of Coherent Atomic Excitation*, John Wiley & Sons, 1990.
86 P. R. Fontana and P. Thomann, *Phys. Rev. A*, 1976, **13**, 1512.
87 J. V. Moloney and W. J. Meath, *Mol. Phys.*, 1975, **30**, 171.
88 W. R. Salzman, *Phys. Rev. Lett.*, 1971, **26**, 220.
89 M. P. Silverman and F. M. Pipkin, *J. Phys. B.*, 1972, **5**, 1844.
90 S. Chelkowski, A. Conjusteau, T. Zuo and A. D. Bandrauk, *Phys. Rev. A*, 1996, **54**, 3235.
91 S. Chelkowski, C. Foisy and A. D. Bandrauk, *Phys. Rev. A*, 1998, **57**, 1176.
92 S. Chelkowski and A. D. Bandrauk, *Laser Phys.*, 2000, **10**, 216.
93 I. Kawata, H. Kono and A. D. Bandrauk, *Phys. Rev. A*, 2001, **6404**, 43411.
94 J. L. Krause, K. C. Kulander, J. C. Light and A. E. Orel, *J. Chem. Phys.*, 1992, **96**, 4283.
95 A. E. Orel and K. C. Kulander, *J. Chem. Phys.*, 1989, **91**, 6086.
96 S. Chelkowski, C. Foisy and A. D. Bandrauk, *Int. J. Quantum Chem.*, 1997, **65**, 503.
97 R. A. Kendall, T. H. Dunning and R. J. Harrison, *J. Chem. Phys.*, 1992, **96**, 6796.
98 T. H. Dunning, *J. Chem. Phys.*, 1989, **90**, 1007.